

Coupled effects of climate variability and land use pattern on surface water quality: An elasticity perspective and watershed health indicators

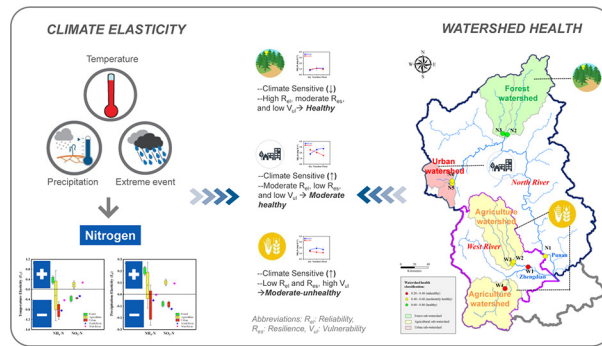
Ayu Ervinia, Jinliang Huang*, Yaling Huang, Jingyu Lin

Coastal and Ocean Management Institute, Xiamen University, Xiamen 361102, China

HIGHLIGHTS

- Climate elasticity of N concentrations varied among land use pattern.
- Forest sub-watersheds had high reliability and resilience, and low vulnerability.
- Disturbed watersheds had high climate elasticity and poor health condition.

GRAPHICAL ABSTRACT



ARTICLE INFO

Article history:
 Received 28 February 2019
 Received in revised form 8 July 2019
 Accepted 24 July 2019
 Available online 25 July 2019

Editor: Ouyang Wei

Keywords:
 Dissolved inorganic nitrogen
 Climate variability
 Land use
 Watershed management
 Coastal watershed

ABSTRACT

Understanding the coupled effects of climate variability and land use on riverine nitrogen is essential for watershed management. The climate–water relationships for ammonium ($\text{NH}_4\text{-N}$) and nitrate ($\text{NO}_3\text{-N}$) were determined by an elasticity approach and then the watershed health index was estimated using the reliability, resilience, and vulnerability framework. These methods were applied to an in-situ monitoring dataset of N concentrations measured during 2010–2017 from nine sub-watersheds in the Jiulong River Watershed, China. The results showed that temperature and precipitation elasticity of $\text{NH}_4\text{-N}$ and $\text{NO}_3\text{-N}$ changed substantially among various land use patterns. The N concentrations were highly sensitive to extreme climate conditions, particularly at urban and agricultural sub-watersheds. The measure of risk indicators revealed that the watershed health index varied from good health to unhealthy status. Linear regression analysis was used to analyze the interactions among watershed characteristics, climate elasticity, and watershed health. Cropland and population had strong positive correlations with climate elasticity of $\text{NO}_3\text{-N}$. Forest and elevation had strong negative associations with climate elasticity of $\text{NO}_3\text{-N}$. Watershed health significantly declined with increasing proportion of cropland and population density. This study demonstrated that human-impacted watersheds were less healthy to unhealthy and tend to be more sensitive to climate variability than natural watersheds, which is useful for efforts aimed at improving watershed management.

© 2019 Elsevier B.V. All rights reserved.

1. Introduction

Riverine dissolved inorganic nitrogen (DIN) is an important indicator in evaluating trophic status of aquatic ecosystem, the health of

* Corresponding author.
 E-mail address: jlhuang@xmu.edu.cn (J. Huang).

watersheds, and effects of multiple stressors in terrestrial and river systems (Greaver et al., 2016; Lu et al., 2017; Mallya et al., 2018). Climate conditions and anthropological N inputs, such as agricultural fertilizer, fossil fuel combustion, and domestic wastewater, are important factors controlling stream N dynamics (Fu et al., 2017; Galloway et al., 2008; Greaver et al., 2016; Kaushal et al., 2011; Paerl, 2006; Wade et al., 2001). Exploring the linkages between climate conditions and water quality and its association with land use is an imperative step to understand how climate change will alter N concentrations, as well as how watershed ecosystems respond to these changes.

Healthy watersheds play a critical role in providing wide array of ecosystem services, such as nutrient cycling, water purification, habitat protection, erosion/sedimentation control, flood control, and climate regulation (Hazbavi et al., 2018). Several studies indicated that land use intensification and climate change have the potential to negatively affect watershed health through increase in hydrologic extremes and contaminant loads from urban and agricultural runoffs (Hoque et al., 2014a; Mehdi et al., 2015). As the U.S. Environmental Protection Agency reported, a healthy watershed will improve resilience to climate change. Towards this, the assessment of watershed health has become particular concerns for developing sustainable practices and climate adaptation strategies to support the achievement of the United Nation's Sustainable Development Goals (SDGs) (Ahn and Kim, 2017; USEPA, 2009). The health assessment has been mainly studied in terms of water quality criteria (Hoque et al., 2012; Mallya et al., 2018). Few studies examined the watershed health by incorporating climate, hydrology, and water quality indicators (Hazbavi et al., 2018; Sadeghi et al., 2019). The comprehensive assessment of ecosystem health at watershed scale helps us to identify priority management areas for mitigation and adaptation to climate change and land use change threats.

Process-based models can be useful determining the climate drives water quality, but the model development can be difficult due to the availability of long-term data input as well as the uncertainty and complexity in parameter calibrations (Whitehead et al., 2006). On the other hand, statistical approaches are commonly used to identify trends and to explore climate-water quality relationship, but they tend to focus on annual trends for the entire watershed (Monteith et al., 2000; Todd et al., 2012). A recent study by Jiang et al. (2014) introduced a concept of climate elasticity of water quality (CEWQ), which is a robust method to describe climate-water quality relationship and overweighs statistical correlations. Climate elasticity of water quality (CEWQ) has been applied in large rivers on global scale (Jiang et al., 2014) and regional scale (Khan et al., 2017). To the best of our knowledge, few studies have examined the sensitivity of water quality to climatic conditions at watershed scales with different dominant land use, such as urban, forest, and agriculture. The assessment at watershed scales could demonstrate local response (i.e. riverine nitrogen) to global change (i.e. climate change and land use change), which is important for local water security. However, the elasticity concept may be too simplistic and unable to delineate the resilience and vulnerability of watersheds to environmental hazards such as climate and land use changes. The watershed health indicators concept has been widely applied to evaluate the effects of climate and land use on water quality by estimating the reliability, resilience, and vulnerability (Hazbavi et al., 2018; Hoque et al., 2014b; Mallya et al., 2018; Sadeghi et al., 2019). Therefore, it should be interesting to integrate the elasticity approach and watershed health indicators to examine the coupled effects of climate variability and land use pattern on the riverine nitrogen.

The Jiulong River Watershed, a coastal watershed in southeast China was selected as the study site to explore the coupled effects of climate variability and watershed land use on riverine nitrogen concentrations. The watershed has experienced intensive land-use change and increased extreme weather events like typhoons in recent few decades (Huang et al., 2013b). The result of a previous study using multiple spatio-temporal scale approach to examine watershed nitrogen exports dynamics across a land-use gradient revealed significant inter-annual

variability of N export (Huang et al., 2018). However, the response of nitrogen concentrations to climate variability is not well understood. It may vary across a land-use gradient. The man-impacted watersheds may be more vulnerable and less resilient to environmental threats than undisturbed watersheds. The objectives of this study are: (1) to investigate the sensitivity of ammonium ($\text{NH}_4\text{-N}$) and nitrate ($\text{NO}_3\text{-N}$) concentrations to intra- and inter- annual climatic (i.e. air temperature and precipitation) variability, (2) to assess the potential watershed health, and (3) to evaluate the relationships among watershed characteristics, climate sensitivity of N concentrations, and watershed health index. The findings of this study can provide a useful insight into the land-climate-water nexus, which is useful for efforts aimed at improving watershed management in other coastal watersheds throughout eastern China.

2. Material and methods

2.1. Study area

The Jiulong River Watershed (JRW) in the eastern of China drains an area of 14,700 km² (Fig. 1). The JRW locates in a subtropical wet climate zone with an annual mean precipitation of 1400–1800 mm and annual mean temperature of 19–21 °C. Precipitation intensity distributes unevenly throughout the year of which 70% occurs between April and September. Two major tributaries, North River and West River with drainage areas of 9560 and 3772 km² converge in Zhangzhou and discharge annual flow of approximately 1200 cubic kilometers into estuarine and coastal waters. The headwater catchment is a mountainous area (almost 70% of watershed has a slope steeper than 18% (Huang et al., 2004). The major geological rock types of the JRW are granite, volcanic tuff, and sandstone whereas the soil types are mainly red earth and lateritic red earth (Cao et al., 2006). Nearly 10 million residents rely upon the water from the Jiulong River for agricultural, domestic, and industrial uses and currently contribute to 25% of Fujian Province's gross domestic product (GDP).

The major land use type in the JRW is: (1) forest land (41.2–94.5%), (2) agriculture land (17.5%), and (3) built-up land (4.5%). Agricultural activities are intensive at the downstream area of Zhangzhou plain. As a typical agriculture watershed, excessive use of chemical fertilizer has been identified as critical non-point source nitrogen pollution in the JRW (Huang and Hong, 2010). This area is also heavily contaminated with industrial and domestic wastewater. The area under this investigation was divided into three types of sub-watersheds: (1) forest sub-watersheds (forest land over 80%), (2) agricultural sub-watersheds (agricultural land over 10%), and (3) urban sub-watersheds (built-up land over 10%). Land use data were adapted from Zhou et al. (2014) in which land categories were generated using a combination of unsupervised classification and spatial reclassification based on manual on-screen digitizing (for details, see Zhou et al., 2014).

2.2. Data collection

The hydro-climatic and nitrogen concentrations data representing 8-year observations from 2010 to 2017 for the Jiulong River Watershed were used for the analysis. Nine sampling sites were selected. Five sites were selected in North River area and 4 sites in West River area. The basic watershed characteristics and land-use proportion of the 9 sampling sites are given in Table 1. Based on our previous study, geology types (i.e., sandstones and siltstones, volcanic rocks) have greater influence on constituent minerals like Ca^{2+} and Mg^{2+} , whereas nutrient concentrations were more related to underlying anthropogenic activities related to land use (non-point and point sources pollution) (Huang et al., 2014; Supplementary, Fig. S3). For this season, we didn't consider the effect of geology in this study. Moreover, we found that land use types were spatially related to soil types in the JRW. Agriculture sub-watersheds were dominated by paddy soil and lateritic red soil,

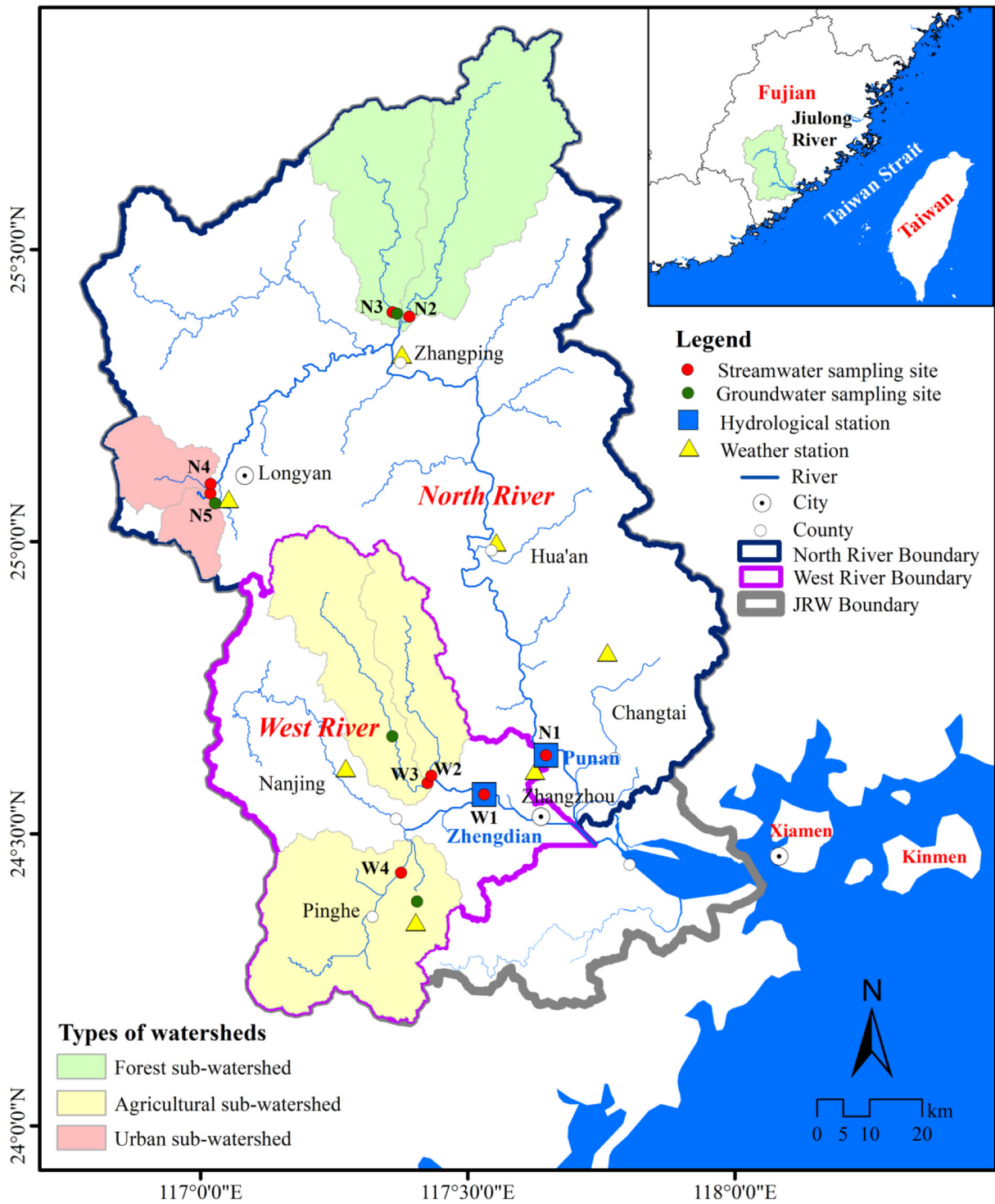


Fig. 1. Map of the Jiulong River Watershed showing the study area, sampling sites (circle), the hydrological stations (square), and weather stations (triangle).

while forest sub-watersheds were comprised mainly by red soil (Supplementary, Table S1). The linkages between soil type and water quality were also consistent with those obtained from land use-water quality relationships (Supplementary, Fig. S4). Therefore, we didn't take soil types into account.

Daily meteorological data including precipitation and air temperature for seven weather stations inside the watershed were acquired from Water Environmental Information System-Jiulong River Basin (<http://47.104.171.193:3506/Index.html#>). The Thiessen Polygon method was applied for determining the average precipitation and

temperature for the individual sub-watersheds. Daily records of river discharge ($m^3 s^{-1}$) at the downstream of the North and West Rivers (Punan and Zhengdian) were obtained from the Hydrological Bureau of Fujian Province. For ungauged sites, the discharge values were estimated by applying The Soil and Water Assessment Tool (SWAT) model that has been calibrated and verified in the Jiulong River Watershed in our previous study (Huang et al., 2013a).

The water samples at the outlet of sub-watersheds were collected during 2010–2017 ($n = 60$ for all sites). Water was sampled three times a year (flood season, dry season, and transition season) during

Table 1
Land use composition and population density for the 9 sampling sites.

Site ID	Name	Area (km ²)	Population density (capita km ⁻²) ^a	Mean elevation (m)	Land use composition ^b		
					Forest (%)	Cropland (%)	Built-up (%)
N5	Suxi	132	201	680	63.1	9.2	27.3
N4	Longmenxi	237	197	680	76.5	9.1	14.1
N3	Shuangyangxi	658	85	650	91.1	7.3	0.9
N2	Xinqiaoxi	972	99	593	93.7	4.4	1.1
N1	Punan	9560	168	616	80.1	16.4	3.6
W4	Huashanxi	1050	531	345	47.4	49.4	2.7
W3	Longshanxi	676	175	507	83.4	13.1	2.8
W2	Yongfengxi	432	156	477	83.0	13.9	1.9
W1	Zhengdian	3772	373	411	67.1	28.0	4.9

^a Population density was derived from Zhangzhou and Longyan Statistical yearbook on 2014.

^b Land use percentages were calculated based on 2010 land use data.

2010–2013. The monthly samples were collected during 2014–2017. In addition to surface water, groundwater samples were also collected from underground wells (depth ~20 m) in April 2018 (n = 4 for three types of sub-watershed). The 25th and 75th percentile values of the monthly streamflow were usually calculated to define these three seasons: dry season (P < 25%), transition season (P = 25%–75%), and flood season (P > 75%) (Huang et al., 2014). Three seasons in the JRW were flood season (Apr, May, Jun, Aug), transition season (Feb, Mar, Jul, Sep, Oct), and dry season (Nov, Dec, Jan). Ammonium (NH₄-N) and nitrate (NO₃-N) were determined following standard methods (SEPCAC, 2002) and completed within 24 h after sampling. The water samples were kept at 4 °C and immediately filtered through 0.45 μm nucleopore membranes prior to N analysis.

Five criteria for watershed health assessment were estimated based on above-mentioned datasets. Table 2 summarized thresholds used for each study criterion for health assessment of the Jiulong River watershed. Each criterion is described as follows:

2.2.1. Standardized Precipitation Index (SPI)

Precipitation has been considered as the main factor controls the formation and persistence of drought and flood. SPI can monitor dry and wet periods over a wide spectrum of time scales from one to 72 months. The SPI was computed using the standardized precipitation-evapotranspiration index (SPEI) package in R program (Vicente-Serrano et al., 2010). To calculate the SPI, the long-term monthly rainfall record was first fitted to a gamma distribution, which was then transformed into a normal distribution. Positive and negative SPI values indicated the precipitation higher and lower than the median of long-term precipitation records, respectively. The SPI values were classified into four categories: normal (0.99 > SPI > -0.99), moderately dry (-1.0 > SPI > -1.49), severely dry (-1.5 > SPI > -1.99), and extremely dry (SPI < -2).

2.2.2. Flow discharges

The hydrological regime is affected by land use change, such as deforestation and urbanization, leading to alteration of runoff responses to rainfall events. Hydrological criteria, such as low (LFD) and high (HFD) flow discharges have been widely used for assessing watershed health. The flow duration curve (FDC) based on the monthly streamflow data was depicted to determine threshold for flow discharge criteria.

Table 2
Thresholds used for each study criterion for health assessment of the Jiulong River watershed.

Criteria	Limit	Description
Standardized precipitation index (SPI)	1	Extracted from CDF of SPI and concluded from WMO (2012).
Low flow discharge (LFD, mm day ⁻¹)	0.50–1.00	Q ₇₅ were derived from the monthly FDC.
High flow discharge (LFD, mm day ⁻¹)	1.65–6.07	Q ₂₅ were derived from the monthly FDC.
Ammonium-N (NH ₄ -N, mg l ⁻¹)	1.9	Chronic criteria magnitude for freshwater aquatic life (USEPA, 2013).
Nitrate-N (NO ₃ -N, mg l ⁻¹)	1.5	The boundary between mesotrophic and eutrophic streams (Dodds et al., 1998).

Two flow discharges that exceeded 75 (Q₇₅) and 25 (Q₂₅) percent of the monthly flow were considered as LFD and HFD thresholds.

2.2.3. Water quality

Eutrophication is a widespread and growing environmental problem that can cause numerous detrimental effects to aquatic life, impair other designated uses, and threaten human health by polluting drinking water supplies (USEPA, 2017). In this study, NH₄-N and NO₃-N were chosen to infer the influence of anthropogenic controls, such as agriculture practices, domestic wastewater, and industrial effluents. Thresholds for water quality criteria are 1.9 mg l⁻¹ for ammonium and 1.5 mg l⁻¹ for nitrate.

2.3. The climate elasticity of water quality

The climate elasticity of water quality (CEWQ) is defined as the proportional change in water quality in response to the proportional change in climatic parameters (i.e., air temperature and precipitation) (Jiang et al., 2014). Temperature elasticity (ε_T) and precipitation elasticity (ε_P) can be calculated using Eqs. (1) and (2):

$$\varepsilon_T = \text{median} \left(\frac{WQ_t - \overline{WQ}}{T_t - \overline{T}} \frac{\overline{T}}{\overline{WQ}} \right) \quad (1)$$

$$\varepsilon_P = \text{median} \left(\frac{WQ_t - \overline{WQ}}{P_t - \overline{P}} \frac{\overline{P}}{\overline{WQ}} \right) \quad (2)$$

where \overline{WQ} , \overline{T} , \overline{P} are the long-term monthly mean water quality, monthly mean air temperature, and monthly mean precipitation, respectively. WQ_t , T_t , and P_t are water quality, air temperature, and precipitation at any given time t , respectively.

The climate elasticity values for NH₄-N and NO₃-N were computed at each site using the monthly time series during the period of 2010–2017.

To estimate ε_T (NH₄-N), the value of $\left(\frac{NH_4-N_t - \overline{NH_4-N}}{T_t - \overline{T}} \frac{\overline{T}}{\overline{NH_4-N}} \right)$ was calculated for each pair of NH₄-N_t and T_t using the monthly time series data set. The median of the aforementioned formula gave the nonparametric estimate of ε_T. Median absolute deviation (MAD) and interquartile range (IQR) were used to check the validity of elasticity values.

CEWQ was classified into four types of elasticity: (1) Inelastic (IE), when the absolute value <0.1; (2) relatively elastic (RE), when $0.1 \leq$ absolute value <0.5; (3) strongly elastic (SE), when absolute value ≥ 0.5 ; and (4) unit elastic (UE), when absolute value was equal to 1.0. Paired-sample *t*-test was applied to evaluate the temperature and precipitation effects ($\alpha = 0.05$) on N concentrations.

In an attempt to compare the pattern of N concentrations under different hydro-climatic conditions, the wet and dry years were chosen regarding the hydrological indices (defined as the division of a hydrological year runoff by mean runoff over the 8 years of study). The wet and dry years had the highest and lowest hydrological index, respectively (1.6 in 2016 and 0.8 in 2017). A linear relationship between runoff and air temperature was established to define time lag between hydro-climatic parameters (Supplementary, Fig. S1). Plots between monthly mean of lagged moving average of air temperature and monthly mean runoff were then depicted (Supplementary, Fig. S2). The mean N concentrations for the dry, flood, and transition seasons in association with watershed types (e.g. forest, urban, and agriculture) during wet and dry years were computed to infer the interactive effects of land-use and climate variability on N concentrations.

2.4. $R_{el}R_{es}V_{ul}$ framework

The watershed health was assessed using the concepts of time-based $R_{el}R_{es}V_{ul}$ conceptual framework (Hashimoto et al., 1982) which provide information on different characteristics of the behavior of a watershed. The $R_{el}R_{es}V_{ul}$ framework proceeded in four steps (Fig. 2), which include criteria selection, threshold selection and computation of failure event, indicators calculations, and watershed health index (WHI) calculation.

Reliability (R_{el}) measures the frequency of failures (Silva, 2010). A failure event was defined when the watershed was failed to function within acceptable limits and thereby leading to an inadequate homeo-static repair mechanism (Lu et al., 2015). From the Eq. (3), reliability was calculated as:

$$Reliability (R_{el}) = \left(1 - \frac{Nr}{N}\right) \tag{3}$$

where Nr is the number of periods when the watershed is not able to meet the study criteria (failure event) and N is the total number of time periods in the analysis. The ratio of Nr to N is therefore the empirical probability of failure of the criteria being met, and R_T is its complement i.e., non-failure probability (Hashimoto et al., 1982; Hoque et al., 2012; Silva, 2010).

The ability of recovery of a watershed from a failure sequence is evaluated by resilience (R_{es}) as defined in Eq. (4). R_{es} characterized the duration of the failure events (Hashimoto et al., 1982; Hoque et al., 2012; Silva, 2010).

$$Resilience(R_{es}) = \frac{N_{fs}}{N_r} \tag{4}$$

where N_{fs} is the total number of failure sequences and N_r has the same meaning as in Eq. (3). The longer the average duration of failure sequences, the more difficult it is for a watershed to recover from a failure (Fowler et al., 2003; Hashimoto et al., 1982; Hoque et al., 2012).

The vulnerability (V_{ul}), characterizes the magnitude of the failure events (Silva, 2010) and measures the severity of failure based on the assumption that the period with the largest failure would be the most severe in terms of its impacts of the study criteria. Thus, V_{ul} was defined as the average of the maximum failure occurring in each continuous failure sequences. In this study, a modified V_{ul} metric was proposed that scales between 0 and 1 as defined in Eq. (5).

$$Vulnerability(V_{ul}) = \frac{1}{N_{fs}} \sum_{k=1}^N \left\{ \left[\frac{X_{obs}(k) - X_{std}}{X_{max} - X_{std}} \right] H[X_{obs}(k) - X_{std}] \right\} \tag{5}$$

$$\left(\left[\frac{X_{std} - X_{obs}(k)}{X_{std} - X_{min}} \right] H[X_{obs}(k) - X_{std}] \text{ in case of LFD} \right)$$

where N_{fs} has the same meaning as in Eq. (4), $X_{obs}(k)$ is the observed study criteria at the k th time step, X_{max} is the maximum value of the observed study criteria, X_{min} is the minimum value of the observed study criteria, X_{std} is the corresponding compliance standard, and H is the Heaviside function that accounts only for failure events and the value is zero for negative argument and one for positive argument (Hashimoto et al., 1982; Hoque et al., 2012; Silva, 2010). It is believed that when deviations of X_{obs} from X_{std} are small $V_{ul} \rightarrow 0$ and when deviations are large $V_{ul} \rightarrow 1$. The value of V_{ul} metric is contrary with those of R_{el} and R_{es} . To make the consistency among three indicators, the negatively sensed index of vulnerability was standardized as:

$$V = 1 - V_{ul} \tag{6}$$

Watershed health index (WHI) based on the $R_{el}R_{es}V_{ul}$ conceptual framework for each sampling sites was computed using the geometric mean as shown in Eq. (7). The geometric mean was selected for the study, because it is more sensitive than other averages to changes in individual variables.

$$WHI = \left[\prod_{i=1}^3 R_{el} \cdot R_{es} \cdot V \right]^{\frac{1}{3}} \tag{7}$$

A watershed health index scored from 0 to 1 and it can be classified in five classes, including very unhealthy (0.00–0.20), unhealthy (0.21–0.40), moderately healthy (0.41–0.60), healthy (0.61–0.80), and very healthy (0.81–1.00).

2.5. Statistical analyses

The linear regression analysis was conducted to examine the relationships between watershed characteristics and climate elasticity of water quality and watershed health index. The watershed

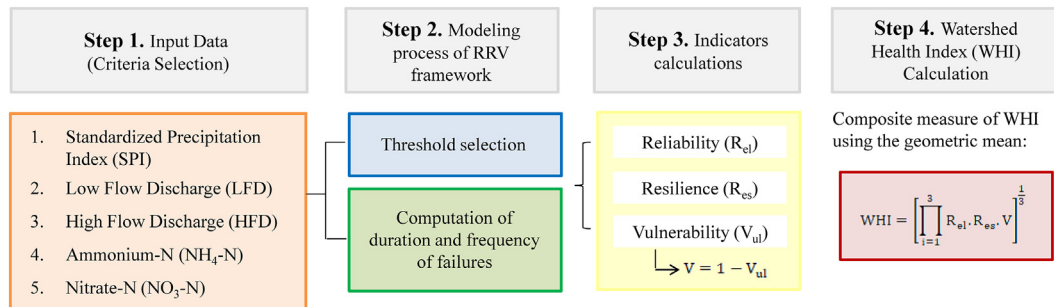


Fig. 2. Four steps of methodology used for the Jiulong River Watershed health assessment.

characteristics considered in this study were % cropland, % forest, % built-up, population density, elevation, and catchment size. The Kolmogorov-Smirnov (K-S) goodness of fit test was performed prior to analysis to check the normality of the distribution of all variables. A variable is normally distributed if significance level is >0.05 . Our analyses suggested that logarithmic transformations of watershed characteristic variables were more appropriate than the raw data (Supplementary, Tables S3–S4). Thus, all analyses were conducted on log-transformed variables data. Two-tailed-F-test was applied to test the significance of the relationships.

3. Results

3.1. Observed N concentrations, climate, and hydrology across catchments

The highest mean monthly $\text{NH}_4\text{-N}$ concentrations were observed in the urban sub-watersheds (1.89 mg N l^{-1}), followed by agricultural sub-watersheds (1.27 mg N l^{-1}) and natural forest sub-watersheds ($0.62 \pm 0.22 \text{ mg N l}^{-1}$) (Table 3). The lowest mean monthly $\text{NO}_3\text{-N}$ concentrations were observed in the forest sub-watersheds (1.03 mg N l^{-1}). For urban and moderately cultivated sub-watersheds (i.e. W2 and W3), the mean monthly $\text{NO}_3\text{-N}$ concentrations were 1.80 and 1.92 mg N l^{-1} , respectively. The intensively cultivated sub-watersheds (W4) had the highest mean nitrate concentration of 9.12 mg N l^{-1} . Nitrogen concentrations in the West River reach were generally higher than those in the North River Reach. Precipitation in the upstream was higher than that in the downstream of the North and West River reaches. The mean specific discharge was higher for agricultural sub-watersheds than those for forest and urban sub-watersheds.

3.2. The climate elasticity of N concentrations

The temperature elasticity (ϵ_T) and precipitation elasticity (ϵ_P) of N concentrations are presented as box plots in Fig. 3. Ammonium-N was positively elastic to temperature and precipitation in forest sub-watersheds, negatively elastic in urban sub-watersheds, and mixed elastic in agricultural sub-watersheds. $\text{NH}_4\text{-N}$ from two reaches of the Jiulong River Watershed, i.e. North River and West River showed negative response to temperature and precipitation. Nitrate-N was positively elastic to temperature and precipitation at agricultural sub-watersheds and West River. Negative elasticity was observed at forest sub-watersheds, urban sub-watersheds, and North River. N concentrations showed strong response to temperature. The response was less significant to precipitation ($p < 0.05$).

The responses of N concentrations to extreme weather conditions (i.e. dry and wet years) are shown in Fig. 4. Ammonium-N were significantly higher in the wet year, particularly during transition and flood seasons ($p < 0.05$). Nitrate-N were also higher in the wet year, but more noticeable during dry and transition seasons ($p < 0.05$). Forest sub-watersheds showed relatively stable N concentrations between

dry and wet years. Concentrations increased during wet year in urban and agricultural sub-watersheds.

3.3. Watershed health index

Table 4 shows the computed reliability, resilience, and vulnerability values for individual driving forces. High R_{el} and R_{es} were estimated for hydro-climatic criteria (i.e. SPI, LFD, and HFD). The lowest R_{el} and R_{es} was estimated for nitrate-N. Flow discharges had the highest V_{ul} . The aggregated $R_{el}R_{es}V_{ul}$ values are in the range of 0.61–0.80 (healthy status) for SPI and ammonium-N, and 0.41–0.60 (moderate health status) for LFD, HFD, and nitrate-N.

Fig. 5 illustrates the spatial variation of watershed health indicators. For reliability indicator (Fig. 5a), sub-watersheds that are predominantly forests are in the range 0.6–0.8. The reliability values decreased to a range 0.4–0.6 in the sub-watersheds with dominant agricultural and urban land uses and North River reach, and even lower in the West River reach. Fig. 5b reveals the agriculturally intensive sub-watersheds and West River reach had low values for resilience, ranging from 0.2 to 0.4. The highest vulnerability was observed at W4 sub-watershed.

The results of the individual risk indicators were integrated to assess the watershed health index (Fig. 5d). WHI was in the range of 0.60–0.80 (good health status) at sub-watersheds that are predominantly forests. WHI deteriorates to a range of 0.4–0.6 (moderately healthy) in the urban and agricultural sub-watersheds. The unhealthiest status was detected at the W4 (Huashan), the sub-watershed drained by approximately 50% of agricultural land use, with WHI value of 0.38. Fig. 5d shows the West River reach was less healthy compared to the North River reach, which might be caused by the intensive agricultural activities resulting in high N inputs to West River watershed.

3.4. Relationships between variables, climate elasticity of N concentrations, and watershed health index

Based on the data shown in the Table 5, the land use, population density, and elevation all have potential impact on climate elasticity of N concentrations and watershed health. Cropland is a significant positive determinant of ϵ_T ($\text{NO}_3\text{-N}$) ($R^2 = 0.71$, $p = 0.004$) and ϵ_P ($\text{NO}_3\text{-N}$) ($R^2 = 0.49$, $p = 0.035$). Built-up was negatively associated with climate elasticity of $\text{NH}_4\text{-N}$ ($p < 0.05$). Forest showed a positive association with ϵ_P ($\text{NH}_4\text{-N}$) and a negative association with ϵ_T ($\text{NO}_3\text{-N}$) and ϵ_P ($\text{NO}_3\text{-N}$) were positively associated with population density, while negatively associated with elevation. As for watershed health index, it shows negative associations with cropland and population density. WHI was positively correlated with forest and elevation, implying the health of watershed health typically improves when forest area increases (Table 5). No significant correlations were found between catchment size and climate water quality sensitivity, and watershed health index.

Table 3
Characteristics of N concentrations, precipitation, temperature, and flow discharge used for the analysis of climate elasticity of N concentrations and watershed health in the Jiulong River Watershed during 2010–2017.

Site	Name	$\text{NH}_4\text{-N}$ (mg N l^{-1})	$\text{NO}_3\text{-N}$ (mg N l^{-1})	Temperature ($^{\circ}\text{C}$)	Precipitation (mm day^{-1})	Specific discharge (mm day^{-1})
N5	Suxi	1.86 ± 1.04	2.04 ± 0.79	20.3 ± 5.70	5.19 ± 4.42	1.32 ± 1.12
N4	Longmenxi	1.94 ± 1.36	1.71 ± 0.85	20.3 ± 5.70	5.19 ± 4.42	1.96 ± 1.67
N3	Shuangyangxi	0.62 ± 0.56	1.06 ± 0.54	21.0 ± 6.01	4.14 ± 3.37	1.92 ± 1.63
N2	Xinqiaoxi	0.55 ± 0.55	0.98 ± 0.45	21.0 ± 6.01	4.14 ± 3.37	2.03 ± 1.69
N1	Punan	0.91 ± 0.66	2.37 ± 0.77	21.0 ± 5.81	4.51 ± 3.48	2.71 ± 1.63
W4	Huashanxi	1.21 ± 0.79	9.12 ± 3.64	21.2 ± 5.54	4.41 ± 3.65	2.16 ± 1.83
W3	Longshanxi	1.74 ± 1.06	2.04 ± 0.81	21.0 ± 5.61	4.81 ± 3.89	1.91 ± 1.72
W2	Yongfengxi	0.72 ± 0.53	1.76 ± 0.55	21.2 ± 5.62	4.60 ± 3.71	2.72 ± 2.39
W1	Zhengdian	1.30 ± 0.74	4.22 ± 1.45	21.2 ± 5.59	4.56 ± 3.68	3.10 ± 1.96

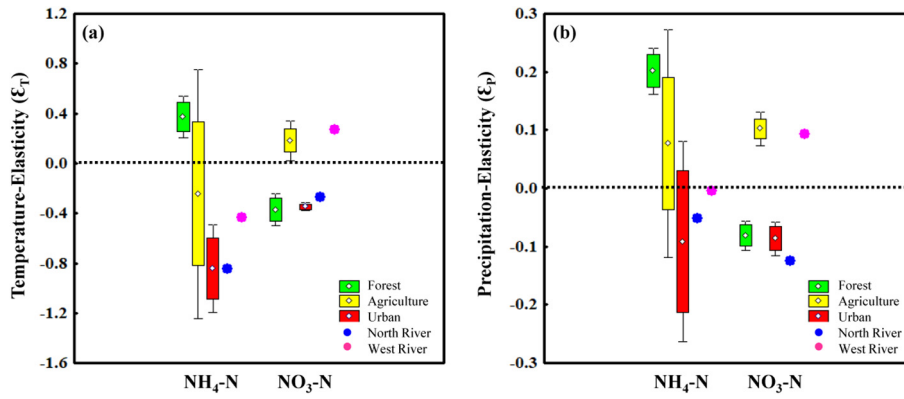


Fig. 3. Temperature and precipitation elasticity of $\text{NH}_4\text{-N}$ and $\text{NO}_3\text{-N}$ concentrations from three types of sub-watersheds and two largest tributaries of Jiulong River Watershed during 2010–2017 (Box: Mean \pm SE; Whisker: Mean \pm SD).

4. Discussion

4.1. The effects of land use on climate-driven seasonality of N concentrations

Climatic drivers can significantly influence intra-annual nitrogen (N) concentrations dynamics through two mechanisms: (1) cycling processes of soil N and (2) hydrologic pathway (Harms and Grimm, 2010; Gascuel-Oudoux et al., 2010). The results of investigation suggest that the climate elasticity of N concentrations varied substantially among three types of watershed according to the variability of N sources. Ammonium-N responds positively to temperature and precipitation at forest sub-watersheds, which indicates the dominant contribution of soil N mineralization. A rise in air temperature is likely to enhance microbial populations controlling mineralization process, while the increase of precipitation resulting in greater soil moistures which can raise the rates of N mineralization (Greaver et al., 2016; Lu et al., 2017; Whitehead et al., 2006). A positive elasticity between nitrate-N and climatic parameters appeared only in the agricultural

sub-watersheds. This is possibly linked to flushing of inorganic $\text{NO}_3\text{-N}$ fertilizer from soil driven by an increase precipitation in flood season. During this period, soil water content is also high along with optimum temperature. This favorable condition is likely to intensify the microbial N transformation (i.e. nitrification), producing quickly nitrate that can be available for transfer to runoff water (Fovet et al., 2018). The synchronous pattern between $\text{NO}_3\text{-N}$ and runoff has been reported in agricultural catchments (Abbott et al., 2018; Álvarez-Cabria et al., 2016; Dupas et al., 2016).

Negative elasticity was observed in urban sub-watersheds where concentrations decreased with increasing temperature and precipitation. The asynchronous pattern between nitrogen and climatic parameters may due to the dilution effects of urban point sources pollution during high flow (Huang et al., 2014). High $\text{NO}_3\text{-N}$ concentrations in the dry and transition seasons suggest the contribution of atmospheric N deposition, as the soil N transformations in urbanized watersheds were limited (Kaushal et al., 2011). Nitrate-N concentrations were low beneath the forest and urban sub-watersheds, indicating limited leaching of nitrate to the groundwater. In contrast, nitrate-N

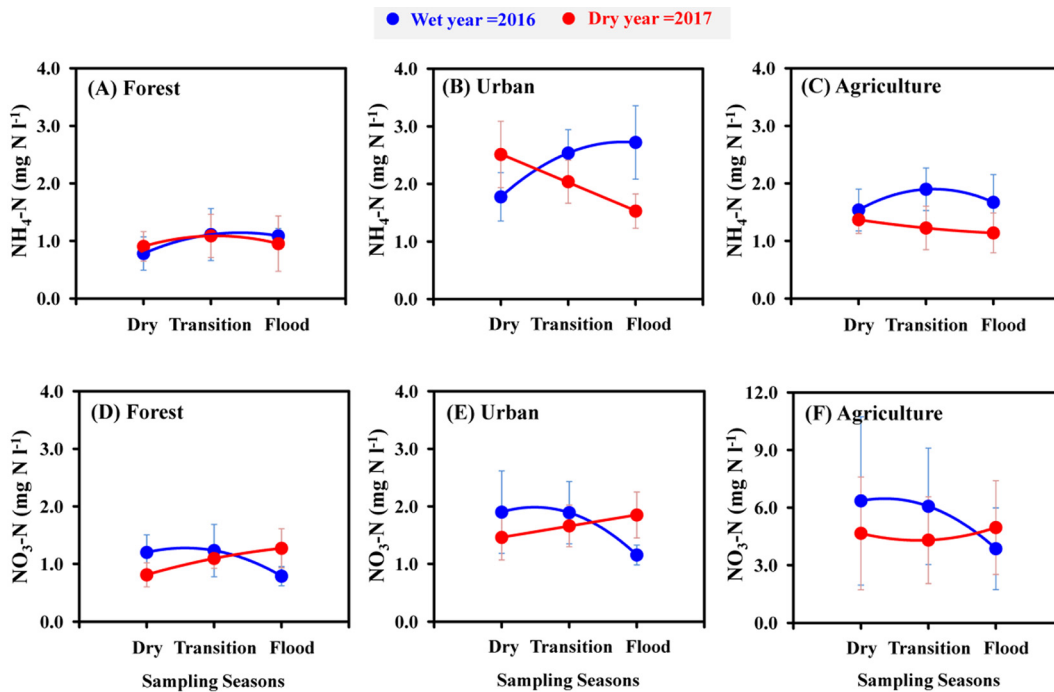


Fig. 4. Comparison of $\text{NH}_4\text{-N}$ and $\text{NO}_3\text{-N}$ concentrations between the three land-use types under contrasting climatic conditions. Each line connects three points which represent sampling seasons (i.e., dry, transition, and flood). Blue symbols represent a wet year (2016) and red symbols represent a dry year (2017). Error bars represent the 95% confidence interval. (For interpretation of the references to colour in this figure legend, the reader is referred to the web version of this article.)

Table 4
Results of $R_{el}R_{es}V_{ul}$ framework for the Jiulong River Watershed during 2010–2017.

Criteria	Reliability (R_{el})	Resilience (R_{es})	Vulnerability (V_{ul})	$R_{el}R_{es}V$
Standardized precipitation index (SPI)	0.72 ± 0.01	0.54 ± 0.09	0.30 ± 0.05	0.65 ± 0.05
Low flow discharge (LFD)	0.76 ± 0.01	0.34 ± 0.09	0.54 ± 0.04	0.49 ± 0.05
High flow discharge (HFD)	0.74 ± 0.01	0.34 ± 0.07	0.40 ± 0.06	0.53 ± 0.05
Ammonium-N (NH_4-N)	0.80 ± 0.18	0.68 ± 0.27	0.13 ± 0.06	0.77 ± 0.17
Nitrate-N (NO_3-N)	0.35 ± 0.33	0.31 ± 0.32	0.15 ± 0.23	0.42 ± 0.30

concentration was very high beneath the agricultural sub-watersheds (Supplementary, Table S2). Results of this investigation reveal the climate related hydrological process determines intra-annual N variation in the urban watersheds, while the microbial activity and N transformations are dominant processes for N cycling in forest and agricultural sub-watersheds.

4.2. Changes in N concentrations during extreme weather conditions (dry vs. wet year)

A large degree of variation in N concentrations under extreme weather conditions is expected since most N transformations and transport are dependent on soil properties and climatic condition (Kaushal

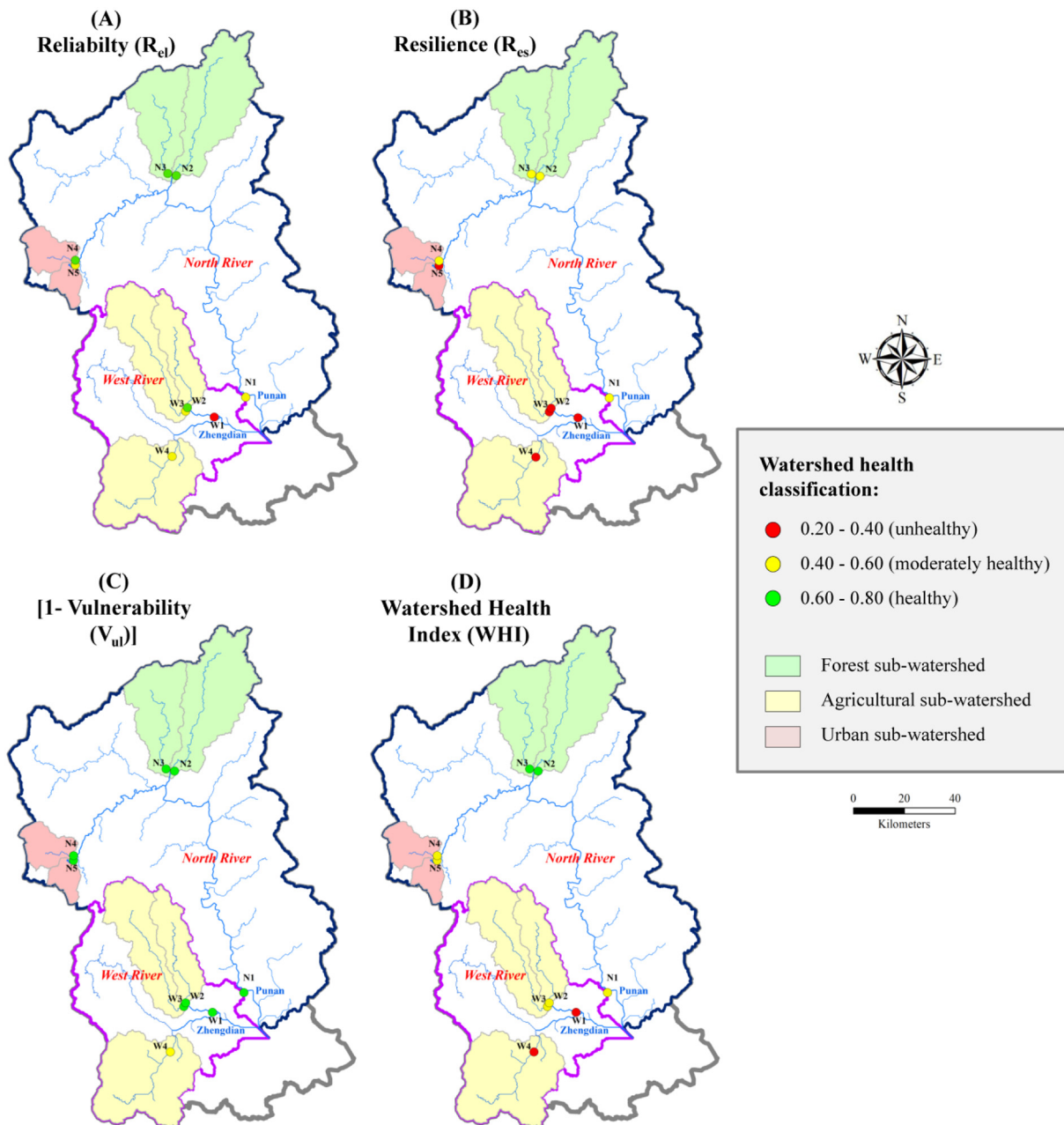


Fig. 5. Spatial distribution of a) Reliability, b) Resilience, c) Vulnerability, and d) Watershed Health Index for the Jiulong River Watershed.

Table 5

Linear regression results between watershed characteristics, climate elasticity of N concentrations, and watershed health index.

Variables		log_cropland	log_builtup	log_forest	log_population	log_elevation	log_catchsize
ε_T (NH ₄ -N)	R ²	0.06	0.467^b	0.160	0.172	0.008	0.003
	p	0.52	0.042	0.286	0.267	0.822	0.897
	β_0^a	0.28	0.219	-6.103	2.323	1.205	-0.146
	β_1^a	-0.25	-0.683	0.4	-0.415	-0.088	-0.051
ε_P (NH ₄ -N)	R ²	0.13	0.567	0.423	0.329	0.001	0.000
	p	0.34	0.019	0.05	0.106	0.940	0.969
	β_0	0.25	0.181	-2.1	0.882	-0.074	0.056
	β_1	-0.36	-0.753	0.65	-0.574	0.029	-0.015
ε_T (NO ₃ -N)	R ²	0.71	0.015	0.263	0.519	0.803	0.073
	p	0.004	0.757	0.158	0.028	0.001	0.482
	β_0	-1.008	-0.056	3.102	-2.093	6.681	-0.519
	β_1	0.845	-0.121	-0.512	0.721	-0.896	0.207
ε_P (NO ₃ -N)	R ²	0.49	0.034	0.228	0.407	0.826	0.006
	p	0.035	0.633	0.194	0.065	0.001	0.844
	β_0	-0.27	0.015	1.014	-0.611	2.348	-0.048
	β_1	0.701	-0.186	-0.477	0.638	-0.909	0.077
WHI	R ²	0.882	0.098	0.650	0.882	0.658	0.068
	p	0.000	0.412	0.009	0.000	0.008	0.498
	β_0	0.85	0.564	-1.062	1.352	-1.414	0.659
	β_1	-0.939	-0.313	0.806	-0.939	0.811	-0.261

Note:

^a Linear regression coefficients $y = \beta_0 + \beta_1 x$.^b Bold font indicates the regression is significant at the p-value < 0.05.

et al., 2008; Lu et al., 2017; Whitehead et al., 1998). This study shows nitrogen concentrations responded strongly to extreme weather conditions, higher concentrations for wet year and lower concentrations for dry year. The runoff also changes greatly with temperature, particularly during transition periods of spring and autumn (Supplementary, Fig. S2). This result agrees with other studies in the United States watersheds that concluded stream nitrogen concentration and export increased with greater runoff and substantially decreased during the drought year (Han et al., 2009; Kaushal et al., 2008; Morse and Wollheim, 2014; Øygarden et al., 2014; Ye and Grimm, 2013). A wet year may drive higher water table, more leaching from nitrogen inputs, and may transport more leached nitrate from soil to stream (Aubert et al., 2013). Increases in rainfall could also enhance soil N processes (e.g. mineralization, nitrification, and denitrification) by microbial activity and therefore positively increase N concentrations in flushing events of the wet year (Whitehead et al., 2009; Ye and Grimm, 2013). A study by Molenat et al. (2008) in the agricultural catchment showed that the catchment become more hydrologically disconnected from the stream under drier conditions. The results of this investigation are in agreement with those findings.

Urban and agricultural sub-watersheds may increase the vulnerability of Jiulong River Watershed to inter-annual climate variability impact on N concentrations. It was found the ammonium concentrations from urban sub-watersheds during the wet year were approximately 2.5 times higher than those from forest sub-watersheds. As expected, nitrate concentrations were greater in the agricultural sub-watersheds, over 5 times higher than value from the forest sub-watersheds during the wet year. The results also suggest that urban and agricultural sub-watersheds may be prone to high nitrogen export during high flow conditions. This vulnerability could result from extensive hydrologic manipulation of sub-urban watersheds that facilitates rapid export of nitrogen that accumulates in dry periods when high flow conditions return. There may also be a limited ability for interaction with biological "hot spots" of denitrification in urban streams during pulses of runoff from impervious surfaces during storms (Kaushal et al., 2008).

4.3. Spatial variation of watershed health index across the JRW

The health of watersheds depends on combination of factors such as land use, topography, climate, soil types, and vegetation (Ahn and Kim, 2017; Sadeghi et al., 2019). The results of this study revealed a high

value (0.61–0.80) of SPI which was based on $R_{el}R_{es}V_{ul}$ index found from the Jiulong River Watershed. The climatic driving force that the JRW is currently in ecologically healthy condition. Such results are in agreement with the results reported by Zhao et al. (2017) that droughts frequencies in Southeast China were relatively lower (<20%) and less serious than that to Northwest China. The SPI based $R_{el}R_{es}V_{ul}$ index from this study was higher than those from a catchment located in Iran, which had the moderate drought severity (Hazbavi et al., 2018). The difference is likely due to the variation in climate dynamics across space. The flow discharges shown in JRW suggests that this watershed is in a moderate health status. This may be due to the variation of intra- and inter-annual rainfall. The $R_{el}R_{es}V_{ul}$ values for ammonium-N and nitrate-N suggest that the JRW is in a good and moderate health status. It is found that fewer ammonium-N concentrations failed to meet the threshold of water quality criteria, compared to nitrate-N concentrations. Many studies have suggested that non-point source pollution from fertilizer application was the major cause of nitrate-N pollution in agricultural watersheds (Aubert et al., 2013; Kaushal et al., 2011).

The results also show that high reliability and resilience, and low vulnerability indicators were found in the forest sub-watersheds. This may be due to the low pollution from the agricultural activities in this area and the effect of purification ability of forest coverage. Some low R_{el} and R_{es} , and high V_{ul} indicators did observe in the sub-watersheds with dominant agricultural and urban land uses, the high pollutant concentrations from agricultural activities may be the reason of high vulnerability. A high V_{ul} indicator for nitrogen has been estimated on agricultural watersheds (Hoque et al., 2014b; Mallya et al., 2018). Other urbanized watersheds investigations (Millington et al., 2015; Shen et al., 2014) had considered urban land as a proxy for point source pollution. This is also the main reason of distress in the watershed hydrological behavior.

This study investigated the watershed health index based $R_{el}R_{es}V_{ul}$ indicators in the JRW varied spatially following the land use gradient. Forest sub-watersheds were considered as healthy, while urban and agricultural sub-watersheds were considered as moderately healthy. The unhealthy condition was detected at W4 (Hushan) and West River reach. It confirmed the finding in other river basins where agricultural and urban watersheds tend to have lower reliability, resilience, and watershed health, and higher values of vulnerability (Hazbavi et al., 2018; Hoque et al., 2014b; Mallya et al., 2018; Sadeghi et al., 2019).

4.4. Factors affecting climate sensitivity of N concentrations and watershed health

The internal characteristics of watersheds can influence the sensitivity of the terrestrial hydrological cycle to large scale climatic forces (Rice et al., 2016). By exploring the relationships among land use, climate sensitivity of water quality, and watershed health, this study may provide useful insight into the climate-land-water nexus. The proportion of cropland is significantly positively correlated with climate elasticity of nitrate, indicating higher impact of climate when agriculture land use is high. The availability of agricultural N inputs and hydrological connectivity could explain the positive correlation. The finding supports prior observations concerning the nitrogen concentrations in agriculture watersheds increased with higher precipitation (Correll et al., 1999; Fukushima et al., 2000; Khan et al., 2017b; Whitehead et al., 2009).

Forest land use showed significant negative correlation with temperature elasticity of nitrate, suggesting that higher forest coverage can decrease the warming impact on nitrate concentration in the JRW. This is similar to the observation made by Monteith et al. (2000) who explained that a rise in air temperature favored the biological uptake of nitrate by terrestrial vegetation, resulting in lower in-stream nitrate concentrations. By contrast, the percentage of forest land is significantly positively correlated with precipitation elasticity of ammonium. The positive correlation indicated that mineralization process enhanced by precipitation and soil wetness from forested lands might be contributing to increased soil ammonium storage (Domisch et al., 2006; Lu et al., 2017). Results of this study were consistent with the previous study that dense riparian vegetation might release substantial amount of ammonium to surface waters because of the organic matter decomposition (Boeder and Chang, 2008).

This study showed that population density was positively correlated to the climate elasticity of nitrate, indicating the response of nitrate concentrations to climate (temperature and precipitation) tends to be stronger in a densely populated area. Most watersheds in China, including the JRW, have limited number of effective wastewater treatment plants. The wastewater with high nutrient concentration was temporarily stored in the catchment and flushed by a heavy rainfall. Therefore, it is reasonable to expect that higher human activities tend to strengthen the response of $\text{NO}_3\text{-N}$ concentrations to climate alterations. Meanwhile, elevation showed the strong negative relationships with climate elasticity of nitrate, implying the watersheds located in the low elevation tend to be more sensitive to climate changes impact on water quality. The elevation gradients may also reflect an effect of land use (Jacobs et al., 2017), given the agricultural activities mainly concentrated in low elevation area of the JRW. Similar finding was given by Nottingham et al. (2015), who reported decline in mineralized $\text{NO}_3\text{-N}$ with elevation is most attributed to temperature constraints on decomposition, biological N fixation, and microbial process at higher elevation.

This study also revealed an insightful contrast between factors-climate sensitivity of N concentrations relationship and factors-watershed health relationship. Forest land use and elevation had strong positive associations with watershed health index, whereas cropland and population density had strong negative associations with watershed health index. This result is consistent with finding of Mallya et al. (2018) who concluded that dilution effects from forest land use may have played a role in improving watershed health condition.

Catchment size revealed no significant impacts on climate sensitivity of N concentrations and watershed health index in the JRW. The effect of catchment area on dissolved inorganic nitrogen (DIN) concentrations is varied from insignificant (Brazier et al., 2007; Gallo et al., 2015) to significant (Jacobs et al., 2017). However, there is some consistency between decreased DIN concentrations with increasing catchment area. These results suggest that increase in catchment area likely stimulates deeper overland flow, and a high river flow can enhance the dilution capacity of the river, leading to a lower concentration of nutrients. Besides, the opportunities for biologically mediated N retention and

cycling also increase at larger catchment scale (Thorp et al., 2006). The results presented here demonstrate the importance of watershed characteristics, as an influence on how changes in water quality occur in response to climate alterations.

4.5. Management implications

The findings of this study provide useful information for efforts aimed at improving watershed management of nitrogen in the Jiulong River Watershed and also to other watersheds in China by considering the interactive effects of climate and land use. It demonstrated the disturbed watersheds experience larger magnitude climate-driven changes in nitrogen concentrations because their internal characteristics, such as intensive agricultural activities, dense population density, and low elevation area, may intensify climate sensitivity. An increased understanding of how internal characteristics of watersheds could mediate the response of nitrogen concentrations to climate changes can potentially be used for the identification of key zones in developing future management plans. The relative disparity of nitrogen between dry and wet year suggests that the widening of "N sinks" landscape is a top priority for the JRW. Implementing best management practices (BMPs), such as stormwater retention ponds, managed wetland, and maintenance of an intact riparian corridor, and green stormwater infrastructure such as green roofs in urban and agricultural watersheds may improve nitrogen retention capacity and counteract the impacts of extreme climate conditions in the JRW. Variation in N concentrations under extreme climate condition indirectly indicated the association between climatic fluctuations and N cycling processes (i.e. mineralization, leaching, denitrification, etc.). This study has some limitations in describing the complex dynamic processes between natural and anthropogenic factors governing the intra- and inter-annual variation of nutrient concentrations in the watershed. However, it is useful as an imperative step to understand the response of riverine nitrogen to dual stressors of climate and land use changes. Therefore, further research using process-based models is required to provide sufficient understanding of the key processes related to N cycling in the JRW.

5. Conclusion

The response of riverine N concentrations to climate stability changed among various watersheds with different dominant land use. Agriculture sub-watersheds were positively elastic, forest sub-watersheds were mixed elastic, while urban sub-watersheds were negatively elastic to climate. Inter-annual variability of N concentrations may be caused by the interactive effects of climate-driven runoff changes and land use patterns. The watershed health assessment revealed that the forest sub-watersheds had higher reliability, resilience, and low vulnerability compared to sub-watersheds with dominant agricultural and urban land use. Interactions were found among internal characteristics of watershed, climate elasticity of water quality, and watershed health. Cropland and population had significant positive associations with climate elasticity and negative association with watershed health. Human activities may increase climate sensitivity and decrease watershed health. Forest coverage and elevation had negative associations with climate elasticity of nitrate and positive association with watershed health. This study demonstrated human-impacted watersheds were less healthy to unhealthy and tend to be more sensitive to climate variability than natural watersheds. Changes in climate conditions and land use pattern are critical to sustainable water resources management.

Acknowledgements

This research was supported by the National Natural Science Foundation of China (Grant No. 41471154), and the Fundamental Research Funds for the Xiamen University (Grant No. 20720150129). Juntao Cai,

Boqiang Huang, Jihui Liu, Cairong Xiao, Hefan Zeng in our research group provided assistance with in-situ monitoring and experiments. We thank Dr. Wang Shih-Chi from the U.S. EPA for his assistance with English writing and anonymous reviewers for constructive feedbacks and comments that helped to improve this paper.

Appendix A. Supplementary data

Supplementary data to this article can be found online at <https://doi.org/10.1016/j.scitotenv.2019.133592>.

References

- Abbott, B.W., Moatar, F., Gauthier, O., Fovet, O., Antoine, V., Ragueneau, O., 2018. Trends and seasonality of river nutrients in agricultural catchments: 18 years of weekly citizen science in France. *Sci. Total Environ.* 624, 845–858. <https://doi.org/10.1016/j.scitotenv.2017.12.176>.
- Ahn, S.R., Kim, S.J., 2017. Assessment of watershed health, vulnerability, and resilience for determining protection and restoration priorities. *Environ. Model. Softw.*, 1–19. <https://doi.org/10.1016/j.envsoft.2017.03.014>.
- Álvarez-Cabria, M., Barquín, J., Peñas, F.J., 2016. Modelling the spatial and seasonal variability of water quality for entire river networks: relationships with natural and anthropogenic factors. *Sci. Total Environ.* 545–546, 152–162. <https://doi.org/10.1016/j.scitotenv.2015.12.109>.
- Aubert, A.H., Gascuel-Odoux, C., Merot, P., 2013. Annual hysteresis of water quality: a method to analyse the effect of intra- and inter-annual climatic conditions. *J. Hydrol.* 478, 29–39. <https://doi.org/10.1016/j.scitotenv.2015.12.109>.
- Boeder, M., Chang, H., 2008. Multi-scale analysis of oxygen demand trends in an urbanizing Oregon watershed, USA. *J. Environ. Manag.* 87, 567–581. <https://doi.org/10.1016/j.jenvman.2007.12.009>.
- Brazier, R.E., Parsons, A.J., Wainwright, J., Powell, D.M., Schlesinger, W.H., 2007. Upscaling understanding of nitrogen dynamics associated with overland flow in a semi-arid environment. *Biogeochemistry* 82, 265–278. <https://doi.org/10.1007/s10533-007-9070-x>.
- Cao, W.Z., Hong, H.S., Zhang, Y.Z., Chen, N.W., Zeng, Y., Wang, W.P., 2006. Anthropogenic nitrogen sources and exports in a village-scale catchment in Southeast China. *Environ. Geochem. Health* 28, 45–51. <https://doi.org/10.1007/s10653-005-9010-4>.
- Correll, D.L., Jordan, T.E., Weller, D.E., 1999. Effects of precipitation and air temperature on nitrogen discharges from Rhode River watersheds. *Water Air Soil Pollut.* 115, 547–575. <https://doi.org/10.1023/A:1005194630598>.
- Dodds, W.K.J., Jones, J.R., Welch, E.B., 1998. Suggested classification of stream trophic state: distributions of temperate stream types by chlorophyll, total nitrogen, and phosphorus. *Water Res.* 32, 1455–1462. [https://doi.org/10.1016/S0043-1354\(97\)00370-9](https://doi.org/10.1016/S0043-1354(97)00370-9).
- Domisch, T., Finér, L., Laine, J., Laiho, R., 2006. Decomposition and nitrogen dynamics of litter in peat soils from two climatic regions under different temperature regimes. *Eur. J. Soil Biol.* 42, 74–81. <https://doi.org/10.1016/j.ejsobi.2005.09.017>.
- Dupas, R., Jomaa, S., Musolff, A., Borchardt, D., Rode, M., 2016. Disentangling the influence of hydroclimatic patterns and agricultural management on river nitrate dynamics from sub-hourly to decadal time scales. *Sci. Total Environ.* 571, 791–800. <https://doi.org/10.1016/j.scitotenv.2016.07.053>.
- Fovet, O., Humbert, G., Dupas, R., et al., 2018. Seasonal variability of stream water quality response to storm events captured using high-frequency and multi-parameter data. *J. Hydrol.* 559, 282–293. <https://doi.org/10.1016/j.jhydrol.2018.02.040>.
- Fowler, H.J., Kilsby, C.G., O'Connell, P.E., 2003. Modeling the impacts of climatic change and variability on the reliability, resilience, and vulnerability of a water resource system. *Water Resour. Res.* 39 (8), 1222. <https://doi.org/10.1029/2002WR001778>.
- Fu, J., Gasche, R., Wang, N., Lu, H., Butterbach-Bahl, K., Kiese, R., 2017. Impacts of climate and management on water balance and nitrogen leaching from montane grassland soils of S-Germany. *Environ. Pollut.* 229, 119–131. <https://doi.org/10.1016/j.envpol.2017.05.071>.
- Fukushima, T., Ozaki, N., Kaminishi, H., et al., 2000. Forecasting the changes in lake water quality in response to climate changes, using past relationships between meteorological conditions and water quality. *Hydrol. Process.* 14, 593–604. [https://doi.org/10.1002/\(SICI\)1099-1085\(20000228\)14:3<593::AID-HYP956>3.0.CO;2-O](https://doi.org/10.1002/(SICI)1099-1085(20000228)14:3<593::AID-HYP956>3.0.CO;2-O).
- Gallo, E.L., Meixner, T., Aoubid, H., Lohse, K.A., Brooks, P.D., 2015. Combined impact of catchment size, land cover, and precipitation on streamflow and total dissolved nitrogen: a global comparative analysis. *Glob. Biogeochem. Cycles* 29, 1109–1121. <https://doi.org/10.1002/2015GB005154>.
- Galloway, J.N., Townsend, A.R., Erisman, J.W., Bekunda, M., Cai, Z., Freney, J.R., Luiz Martinelli, L.A., Seitzinger, S.P., Sutton, M.A., 2008. Transformation of the nitrogen cycle: recent trends, questions, and potential solutions. *Science* 320, 889–892. <https://doi.org/10.1126/science.1136674>.
- Gascuel-Odoux, C., Aourousseau, P., Durand, P., Ruiz, L., Molenat, J., 2010. The role of climate on inter-annual variation in stream nitrate fluxes and concentrations. *Sci. Total Environ.* 408 (2010), 5657–5666. <https://doi.org/10.1016/j.scitotenv.2009.05.003>.
- Greaver, T.L., Clark, C.M., Compton, J.E., Vallano, D., Talhelm, A.F., Weaver, C.P., Band, L.E., Baron, J.S., Davidson, E.A., Tague, C.L., Felker-Quinn, E., Lynch, J.A., Herrick, J.D., Liu, L., Goodale, C.L., Novak, K.J., Haeuber, R.A., 2016. Key ecological responses to nitrogen are altered by climate change. *Nat. Clim. Chang.* 6, 836–843. <https://doi.org/10.1038/nclimate3088>.
- Han, H., Allan, J.D., Scavia, D., 2009. Influence of climate and human activities on the relationship between watershed nitrogen input and river export. *Environ. Sci. Technol.* 43, 1916–1922. <https://doi.org/10.1021/es801985x>.
- Harms, T.K., Grimm, N.B., 2010. Influence of the hydrologic regime on resource availability in a semi-arid stream riparian corridor. *Ecohydrol* 3, 349–359. <https://doi.org/10.1002/eco.119>.
- Hashimoto, T., Loucks, D.P., Stedinger, J., 1982. Reliability, resilience and vulnerability for water resources system performance evaluation. *Water Resour. Res.* 18, 14–20. <https://doi.org/10.1029/WR018i001p00014>.
- Hazbavi, Z., Keesstra, S.D., Nunes, J.P., Baartman, J.E.M., Gholamalifard, M., Sadeghi, S.H., 2018. Health comparative comprehensive assessment of watersheds with different climates. *Ecol. Indic.* 93, 781–790. <https://doi.org/10.1016/j.ecolind.2018.05.078>.
- Hoque, Y.M., Tripathi, S., Hantush, M.M., Govindaraju, R.S., 2012. Watershed reliability, resilience and vulnerability analysis under uncertainty using water quality data. *J. Environ. Manag.* 10, 101–112. <https://doi.org/10.1016/j.jenvman.2012.05.010>.
- Hoque, Y.M., Raj, C., Hantush, M.M., Chaubey, I., Govindaraju, R.S., 2014a. How do land-use and climate change affect watershed health? A scenario-based analysis. *Water Qual Expo Health* 6, 19–33. <https://doi.org/10.1007/s12403-013-0102-6>.
- Hoque, Y.M., Hantush, M.M., Govindaraju, R.S., 2014b. On the scaling behavior of reliability-resilience-vulnerability indices in agricultural watersheds. *Ecol. Indic.* 40, 136–146. <https://doi.org/10.1016/j.ecolind.2014.01.017>.
- Huang, J.L., Hong, H.S., 2010. Comparative study of two models to simulate diffuse nitrogen and phosphorus pollution in a medium-sized watershed, southeast China. *Estuar. Coast. Shelf Sci.* 86, 387–394. <https://doi.org/10.1016/j.ecss.2009.04.003>.
- Huang, J.L., Hong, H.S., Zhang, L.P., 2004. Study on predicting soil erosion in Jiulong River watershed based on GIS and USLE. *J. Soil Water Conserv.* 18, 75–79 (in Chinese).
- Huang, J.L., Zhou, P., Zhou, Z.R., Huang, Y.L., 2013a. Assessing the influence of land use and land cover datasets with different points in time and levels of detail on watershed modeling in the North River watershed, China. *Int. J. Environ. Res. Public Health* 10, 144–157. <https://doi.org/10.3390/ijerph10010144>.
- Huang, J.L., Zhang, Z.Y., Feng, Y., Hong, H.S., 2013b. Hydrologic response to climate change and human activities in a subtropical coastal watershed of southeast China. *Reg. Environ. Chang.* 13, 1195–1210. <https://doi.org/10.1007/s10113-013-0432-8>.
- Huang, J.L., Huang, Y.L., Zhang, Z.Y., 2014. Coupled effects of natural and anthropogenic controls on seasonal and spatial variations of river water quality during baseflow in a coastal watershed of Southeast China. *PLoS One* 9 (3), 1–19. <https://doi.org/10.1371/journal.pone.0091528>.
- Huang, Y.L., Huang, J.L., Ervinia, A., Duan, S., Kaushal, S.S., 2018. Land use and climate variability amplifies watershed nitrogen exports in coastal China. *Ocean Coast. Manag.* <https://doi.org/10.1016/j.ocecoaman.2018.02.024>.
- Jacobs, S.R., Breuer, L., Butterbach-Bahl, K., Pelster, D.E., Rufino, M.C., 2017. Land use affects total dissolved nitrogen and nitrate concentrations in tropical montane streams in Kenya. *Sci. Total Environ.* 603–604, 519–532. <https://doi.org/10.1016/j.scitotenv.2017.06.100>.
- Jiang, J., Sharma, A., Sivakumar, B., Wang, P., 2014. A global assessment of climate-water quality relationships in large rivers: an elasticity perspective. *Sci. Total Environ.* 468–469 (2014), 877–891. <https://doi.org/10.1016/j.scitotenv.2013.09.002>.
- Kaushal, S.S., Groffman, P.M., Band, L.W., Shields, C.A., Morgan, R.P., Palmer, M.A., Belt, K.T., Swan, C.M., Findlay, S.E.G., Fisher, G.T., 2008. Interaction between urbanization and climate variability amplifies watershed nitrate export in Maryland. *Environ. Sci. Technol.* 42, 5872–5878. <https://doi.org/10.1021/es800264f>.
- Kaushal, S.S., Groffman, P.M., Band, L.E., Elliott, E.M., Shields, C.A., Kendall, C., 2011. Tracking nonpoint source nitrogen pollution in human-impacted watersheds. *Environ. Sci. Technol.* 45, 8225–8232. <https://doi.org/10.1021/es200779e>.
- Khan, A.U., Jiang, J., Sharma, A., Wang, P., Khan, J., 2017b. How do terrestrial determinants impact the response of water quality to climate drivers? An elasticity perspective on the water-land-climate nexus. *Sustainability* 9, 1–20. <https://doi.org/10.3390/su9112118>.
- Lu, Y., Wang, R., Zhang, Y., Su, H., Wang, P., Jenkins, A., Ferrier, R.C., Bailey, M., Squire, G., 2015. Ecosystem health towards sustainability. *Ecosyst. Health Sustain.* 1 (1), 1–15. <https://doi.org/10.1890/EHS14-0013.1>.
- Lu, M.C., Chang, C.T., Lin, T.C., Wang, L.J., Wang, C.P., Hsu, T.C., Huang, Jr-C, 2017. Modeling the terrestrial N processes in a small mountain catchment through INCA-N: a case study in Taiwan. *Sci. Total Environ.* 593–594, 319–329. <https://doi.org/10.1016/j.scitotenv.2017.03.178>.
- Mallya, G., Hantush, M., Govindaraju, R.S., 2018. Composite measures of watershed health from a water quality perspective. *J. Environ. Manag.* 214, 104–124. <https://doi.org/10.1016/j.jenvman.2018.02.049>.
- Mehdi, B., Ludwig, R., Lehner, B., 2015. Evaluating the impacts of climate change and crop land use change on streamflow, nitrates, and phosphorus: a modeling study in Bavaria. *J. Hydrol. Reg. Stud.* 4, 60–90. <https://doi.org/10.1016/j.ejrh.2015.04.009>.
- Millington, H.K., Lovell, J.E., Lovell, C.A.K., 2015. A framework for guiding the management of urban stream health. *Ecol. Econ.* 109, 222–233. <https://doi.org/10.1016/j.ecolecon.2014.11.017>.
- Molenat, J., Gascuel-Odoux, C., Ruiz, L., Gräu, G., 2008. Role of water table dynamics on stream nitrate export and concentration. In agricultural headwater catchment (France). *J. Hydrol.* 348 (3–4), 363–378. <https://doi.org/10.1016/j.jhydrol.2007.10.005>.
- Monteith, D.T., Evans, C.D., Reynolds, B., 2000. Are temporal variations in the nitrate content of UK upland freshwaters linked to the North Atlantic Oscillation? *Hydrol. Process.* 14, 1745–1749. [https://doi.org/10.1002/1099-1085\(200007\)14:10<1745::AID-HYP116>3.0.CO;2-O](https://doi.org/10.1002/1099-1085(200007)14:10<1745::AID-HYP116>3.0.CO;2-O).
- Morse, N.B., Wollheim, W.M., 2014. Climate variability masks the impacts of land use change on nutrient export in a suburbanizing watershed. *Biogeochemistry* 121,

- 45–59. <https://doi.org/10.1007/s10533-014-9998-6>.
- Nottingham, A.T., Turner, B.L., Whitaker, J., Ostle, N.J., McNamara, N.P., Bardgett, R.D., Salinas, N., Meir, P., 2015. Soil microbial nutrient constraints along a tropical forest elevation gradient: a belowground test of a biogeochemical paradigm. *Biogeosciences* 12, 6071–6083. <https://doi.org/10.5194/bg-12-6071-2015>.
- Øygarden, L., Deelstra, J., Lagzdins, A., Bechmann, M., Greipsland, I., Kyllmar, K., Povilaitis, A., Iital, A., 2014. Climate change and the potential effects on runoff and nitrogen losses in the Nordic-Baltic region. *Agric. Ecosyst. Environ.* 198, 114–126. <https://doi.org/10.1016/j.agee.2014.06.025>.
- Paerl, H.W., 2006. Assessing and managing nutrient-enhanced eutrophication in estuarine and coastal waters: interactive effects of human and climatic perturbations. *Ecol. Eng.* 26, 40–54. <https://doi.org/10.1016/j.ecoleng.2005.09.006>.
- Rice, J.S., Emanuel, R.E., Vose, J.M., 2016. The influence of watershed characteristics on spatial patterns of trends in annual scale streamflow variability in the continental U.S. *J. Hydrol.* 540, 850–860. <https://doi.org/10.1016/j.jhydrol.2016.07.006>.
- Sadeghi, S.H., Hazbavi, Z., Gholamalifard, M., 2019. Interactive impacts of climate, hydrologic, and anthropogenic activities on watershed health. *Sci. Total Environ.* 648, 880–893. <https://doi.org/10.1016/j.scitotenv.2018.08.004>.
- Shen, Z., Hou, X., Li, W., Aini, G., 2014. Relating landscape characteristics to non-point source pollution in a typical urbanized watershed in the municipality of Beijing. *Landsc. Urban Plan.* 123, 96–107. <https://doi.org/10.1016/j.landurbplan.2013.12.007>.
- Silva, A.T., 2010. Design of the Storage Capacity of Artificial Reservoirs. Dissertation of Master in Civil Engineering, October 2010. Instituto Superior Tecnico, Universidade Tecnica Lisboa 104 pp. http://www.civil.ist.utl.pt/~mps/Mod_hid/Teoria/Thesis%20about%20reservoir%20design%20-%20Artur%20Tiago%20Silva.pdf.
- State Environmental Protection Administrator of China (SEPA), 2002. *Methods of Monitoring and Analyzing for Water and Wastewater*. fourth ed. Chinese Environment Science Press.
- Thorpe, J.H., Thoms, M.C., Delong, M.D., 2006. The riverine ecosystem synthesis: biocomplexity in river networks across space and time. *River Res. Appl.* 22, 123–147. <https://doi.org/10.1002/rra.901>.
- Todd, A.S., Manning, A.H., Verplanck, P.L., Crouch, C., McKnight, D.M., Dunham, R., 2012. Climate-change-driven deterioration of water quality in a mineralized watershed. *Environ. Sci. Technol.* 46, 9324–9332. <https://doi.org/10.1021/es3020056>.
- United States Environmental Protection Agency (USEPA), 2009. EPA healthy watersheds program: integrating watershed assessment and protection across EPA. https://www.epa.gov/sites/production/files/2015-10/documents/2009_08_05_nps_healthywatersheds_highquality_hwi.pdf.
- United States Environmental Protection Agency (USEPA), 2013. *Aquatic Life Ambient Water Quality Criteria for Ammonia-Freshwater*. Office of Water, Office of Science and Technology, Washington, DC (242 pp.). <https://www.epa.gov/sites/production/files/2015-08/documents/aquatic-life-ambient-water-quality-criteria-for-ammonia-freshwater-2013.pdf>.
- United States Environmental Protection Agency (USEPA), 2017. *Water quality standards handbook, chapter 3: water quality criteria*. <https://www.epa.gov/sites/production/files/2014-10/documents/handbook-chapter3.pdf>.
- Vicente-Serrano, S.M., Beguería, S., López-Moreno, J.L., 2010. A multi-scalar drought index sensitive to global warming: the standardized precipitation evapotranspiration index-SPEI. *J. Clim.* 23, 1696. <https://doi.org/10.1175/2009JCLI2909.1>.
- Wade, A.J., Soulsby, C., Langan, S.J., Whitehead, P.G., Edwards, A.C., Butterfield, D., Smart, R.P., Cook, Y., Owen, R.P., 2001. Modelling instream nitrogen variability in the Dee catchment, NE Scotland. *Sci. Total Environ.* 265, 229–252. [https://doi.org/10.1016/S0048-9697\(00\)00661-6](https://doi.org/10.1016/S0048-9697(00)00661-6).
- Whitehead, P.G., Wilson, E.J., Butterfield, D., Seed, K., 1998. A semi-distributed integrated flow and nitrogen model for multiple source assessment in catchments (INCA): part II-application to large river basins in South Wales and eastern England. *Sci. Total Environ.* 210–211, 559–583. [https://doi.org/10.1016/S0048-9697\(98\)00038-2](https://doi.org/10.1016/S0048-9697(98)00038-2).
- Whitehead, P.G., Wilby, R.L., Butterfield, D., Wade, A.J., 2006. Impacts of climate change on in-stream nitrogen in a lowland chalk stream: an appraisal of adaptation strategies. *Sci. Total Environ.* 365, 260–273. <https://doi.org/10.1016/j.scitotenv.2006.02.040>.
- Whitehead, P.G., Wilby, R.L., Battarbee, R.W., Kernan, M., Wade, A.J., 2009. A review of the potential impacts of climate change on surface water quality. *Hydrol. Sci.* 54, 101–122. <https://doi.org/10.1623/hysj.54.1.101>.
- World Meteorological Organization, 2012. *Standardized Precipitation Index User Guide* (M. Svodoba, M. Hayes, and D. Wood). (WMO-No.1090), Geneva. http://www.wamis.org/agm/pubs/SPI/WMO_1090_EN.pdf.
- Ye, L., Grimm, N.B., 2013. Modelling potential impacts of climate change on water and nitrate export from a mid-sized, semiarid watershed in the US Southwest. *Clim. Chang.* 120, 419–431. <https://doi.org/10.1007/s10584-013-0827-z>.
- Zhao, S., Cong, D., He, K., Yang, H., Qin, Z., 2017. Spatial-temporal variation of drought in China from 1982 to 2010 based on a modified Temperature Vegetation Drought Index (mTVDI). *Sci. Rep.* 7, 17473 1–12. <https://doi.org/10.1038/s41598-017-17810-3>.
- Zhou, P., Huang, J.L., Pontius, R.G., Hong, H.S., 2014. Land classification and change intensity analysis in a coastal watershed of Southeast China. *Sensors* 14, 11640–11658. <https://doi.org/10.3390/s140711640>.